



Published in final edited form as:

Acta Biomater. 2010 December ; 6(12): 4734–4742. doi:10.1016/j.actbio.2010.07.003.

3D Scaffold of Electrospayed Fibers with Large Pore Size for Tissue Regeneration

Jong Kyu Hong and Sundararajan V. Madihally*

School of Chemical Engineering, Oklahoma State University, 423 Engineering North, Stillwater, OK 74078

Abstract

Regeneration of tissues using biodegradable porous scaffolds has been an intensely investigated area. Since electrospinning can produce scaffolds mimicking nanofibrous architecture found in the body, it recently has gained widespread attention. However, a major problem is the lack of pore size necessary for infiltration of cells into the layers below the surface, restricting cell colonization to the surfaces only. This study describes a novel twist to the traditional electrospinning technology. In particular, collector plates are designed which allows forming very thin layers with pore sizes suitable for cell infiltration. Thin samples can be handled without mechanically damaging the structure and can be transferred into cell culture. These thin layers were stacked by layer-by-layer assembly to develop thick structures. Thirty day cultures of fibroblasts show attachment and spreading of cells in every layer. This concept is useful in regenerating thick tissues with uniformly distributed cells and others in vitro cell culture.

1. INTRODUCTION

Tissue engineering or regeneration focuses on restoring, maintaining, and enhancing tissue and organ function [1]. In tissue engineering, biodegradable scaffolds are used to support and guide cells to proliferate, organize and produce their own extracellular matrix (ECM)[2] and scaffolding material eventually disappears, leaving only the necessary healthy tissue in a topologically required form [3]. A biomimic matrix for cell growing is a fundamental element for tissue regeneration. Templates generated from natural [4] and synthetic polymers or after removing the cellular components from xenogeneic tissues [5] have been used to support and guide the in-growth of cells. Synthesizing scaffolds using techniques such as controlled rate freezing and lyophilization [6], porogen-leaching technique [7], gas-foaming technique[8], microfabrication [9], and free-form printing [10] has gained more attention. Although each technique has advantages and disadvantages, electrospinning technique has recently emerged as a novel technique for tissue regeneration because it allows fabrication of nano and micro size fibers, which are very similar to the characteristic of natural extracellular environment.

The process of fabricating synthetic fibers (nm- μ m) with non-woven structures using electrostatic forces, called electrospinning (electrospray and spinning) has been known for over 100 years. Although electrospinning technology was first patented in the US in 1902[11], this technology was latent until the era of nanoscience and nanotechnology in the 1990s. The

*Corresponding address: 423 Engineering North, School of Chemical Engineering, Oklahoma State University, Stillwater, OK 74078, Ph: (405) 744 9115, FAX: (405) 744 6338, sundar.madihally@okstate.edu.

Publisher's Disclaimer: This is a PDF file of an unedited manuscript that has been accepted for publication. As a service to our customers we are providing this early version of the manuscript. The manuscript will undergo copyediting, typesetting, and review of the resulting proof before it is published in its final citable form. Please note that during the production process errors may be discovered which could affect the content, and all legal disclaimers that apply to the journal pertain.

electrospinning process is versatile and its productivity higher than other methods of fabrication of nanofibers. With a suitable polymer and appropriate solvent system, fiber size can be controlled by manipulating process parameters (40 nm to 10 μm). Since the technology allows the possibility of tailoring the mechanical and biological properties, there has been a significant effort to adapt the technology for use in tissue regeneration [12–13]. Most soluble polymers with high molecular weight can be electrospayed (fibers collected on a stationary collector plate) or electrospun. Nanofibers can be made of natural and synthetic polymers, and polymer blends.

A major problem in electrospinning technology is the lack of generating structural features necessary for building three-dimensional (3D) tissues [12,14]. The pore sizes are less than 10 μm , while human cells are typically greater than 10 μm in size [15]. Hence, cell growth is restricted to the surface only. The reduced pore size is primarily due to multiple layers of fibers deposited to obtain thicker structures that withstand mechanical handling in subsequent steps. Addressing the cell seeding problem by depositing both the polymer as well as cells simultaneously is a recent advancement [16]. However, this approach is not practical as cells will be exposed to a) toxic organic solvents used in the process, b) high shear rates induced by the flow of fluids through narrow nozzles, and c) sub-optimal environmental conditions during manufacturing. These factors affect cell viability and growth function tissue growth. Due to reduced pore size and restricted cell infiltration, it is not possible to regenerate tissues of a thickness suitable for clinical transplantation.

In this study, we introduce an innovative electrospaying technique with a novel collector plate which allows the formation of very thin layers of micro- and nanofibers. Due to reduced thickness, pore size ($\sim 60 \mu\text{m}$) of the formed layers is suitable for mammalian cell infiltration. We performed the fibroblast cell culture of multiple layers using layer-by-layer assembly: place one layer of thin fibers, seed cells and repeat. We show the 3D scaffolds of thin layers of electrospayed fibers in which human fibroblasts are growing not only horizontally but also vertically due to large pore sizes of electrospayed fibers. The implications of the 3D scaffold with layer-by-layer technique will expand to other cells, fibers, tissues and organs, and becomes a phenotype of 3D scaffolds in tissue regeneration.

2. MATERIALS AND METHOD

2.1. Materials

Polycaprolactone (PCL, $M_n=80,000$) and Gelatin Type A were purchased from Sigma (St, Louis, MO) and PCL ($M_w=43,000-50,000$) was obtained from Polysciences (Warrington, PA). Chloroform, methanol, and acetic acid were purchased from Pharmco (Brookfield, CT). For cell culture study, Human foreskin fibroblast (HFF-1) was obtained from American Type Culture Collection (ATCC, Walkersville, MD). Dulbecco's modified Eagle Medium (DMEM), glucose and amphotericin B were obtained from Sigma (St, Louis, MO). Fetal bovine serum (FBS), Alexa Fluor 546 and 4',6-diamidino-2-phenylindole (DAPI) were purchased from Invitrogen (Carlsbad, CA). TrypLE Express, penicillin-streptomycin, and L-glutamine were obtained from Gibco (Grand Island, NY) and sodium bicarbonate was purchased from EMD (Gibbstown, NJ).

2.2. Fabrication of the thin layer of electrospayed fibers

Electrospaying apparatus consisted of a syringe pump (74900 series, Cole-Parmer Instrument Company, Vernon Hills, IL), BD 10 mL syringe (Luer-Lok Tip; Becton Dickinson and Company, Franklin Lakes, NJ), needle tip, high voltage power supply (ES30P-5W/DAM, Gamma high Voltage Research, Ormond Beach, FL), earth grounding, and a collector plate (Figure 1A). The novel collector had four holes (diameter, 1.9 cm and depth 1.2 cm) in a

wooden frame (3cm × 10cm × 2 cm) wrapped with aluminum foil (Figure 1E). The conventional collector plate of the same size as the novel collector without a hole was wrapped with aluminum foil. Electrospayed fibers were fabricated at 40 mL/hr and 20 kV. For micro-sized fibers, 20% (wt/v) PCL ($M_w=43,000-50,000$) dissolved in a mixture solvent of chloroform and methanol (mixing ratio 9 to 1), was sprayed using a 14G needle. The distance of the collector plate was 12 cm from the tip of the needle. For nano-sized fibers, 10% (wt/v) PCL dissolved in a mixture solvent of chloroform and methanol (mixing ratio 9 to 1) was sprayed using a 26 G needle. The distance of the collector plate was 15 cm from the tip of the needle. Deposit volume of the solution was 0.75 mL. Gelatin fibers were formed using 20% (wt/v) gelatin dissolved in acetic acid and distilled water (mixing ratio 7 to 3). Flow rate, needle size, high voltage supply and distance between the needle tip and the collector were 10 ml/hr, 20G, 10kV, and 8cm.

For simultaneous and sequential deposit, 20 w/v% PCL ($M_n=80,000$) was prepared with a solvent mixture of chloroform and methanol (mixing ratio 9 to 1). In the simultaneous and the sequential processes, fibers were formed at the same condition described for gelatin fiber formation using the novel collector.

2.3. Microstructure characterization

Samples were analyzed using JEOL 6360 (Jeol USA Inc., Peabody, MA) at an accelerated voltage of 9 to 20 kV similar to our previous publications [17]. In brief, samples were attached to an aluminum stub using a conductive graphite glue (Ted Pella Inc., Redding, CA) and sputter-coated with gold for 1 minute before SEM study.

Along with the obtained SEM images, fiber diameters, pore size and shape factors of pores ($4\pi \times \text{area} / \text{perimeter}^2$, when the number is closer to 1, the cell shape is closer to a circle) were quantified using Sigma Scan Pro (SPSS Science, Chicago, IL). More than 35 points of fibers and pores were analyzed.

2.4. Mechanical test

Micro size fibers were fabricated using a collector plate (10cm × 3.5cm × 2cm) with a rectangular hole (5cm × 1cm × 1 cm) had an additional flat surface area or peripheral area of a rectangular hole, resulting in two rectangular holes (one with a flat surface and the other without). Fibers accumulated in the flat surface were used as samples for conventional fibers while the fibers collected in the hole were used as samples for novel fibers. Tensile testing was performed at room temperature with dry conditions by the method previously described [18]. In brief, 25 mm (width) × 10 mm (length) rectangular strips were cut from novel and conventional sample and strained to break at a constant crosshead speed of 10 mm/min using INSTRON 5542 (INSTRON, Canton, MA).

2.5. Cell culture

HFF-1 was cultured in DMEM supplemented with 4 mM L-glutamine, 4.5 g/L glucose, 1.5 g/L sodium bicarbonate, 100 U/mL penicillin-streptomycin, 2.5 mg/mL amphotericin B, and 15% FBS. The cells were maintained in CO₂ incubator at 37 °C. The media was changed every 2 days. Before cell seeding, cells were detached with 2% TrypLE Express, centrifuged, and suspended in serum-added media.

Microsize fibers were fabricated using 20 w/v% of PCL ($M_w=43000$) in chloroform/methanol (ratio 9 to 1) and the novel collector. Flow rate, needle size, high voltage supply and distance between the needle tip and the collector were 10 ml/hr, 20G, 10kV, and 8cm. The deposit volume was 0.75mL. Fibers on the aluminum frame were sterilized using UV light for 4 hours, immersed in ethanol for 4 hours, and rinsed by PBS three times. The thin layers were soaked

in serum added media for 4 hours. The cell culture plates were treated with albumin to minimize cell adhesion to the tissue culture plastic surface prior to insertion of a thin layer of fibers (Figure 2). Then, 30,000 cells in 100 μ L were seeded onto 5 points of fibers in a single layer of the aluminum frame.

For three layer cultures, the cell culture in the single layer was repeated three times by using layer-by-layer technique: place one layer of the sample, seed cells on five points of the sample and repeat the process of sample loading and cell seeding two more times. Ten minutes after cell-seeding, 2 and 3 mL of media were added into 6 well plates for single and three layers, respectively.

2.6. Evaluating of cell distribution and organization

At 1, 4 and 7 days after cell culture, the sample was fixed with 3.7% formaldehyde, rinsed with PBS, and immersed in ethanol at -20°C . Then, the sample was stained with 2 mL of Alexa phalloidin (0.66 μM) for cytoskeletal actin and counterstained with 2 mL of DAPI (30 nmol) for nuclei of cells, respectively [19]. The samples were first observed under an inverted fluorescence microscope (Nikon TE2000, Melville, NY). Digital micrographs were collected using a CCD camera. The data were treated using Corel Paint Shop Pro Photo X2 to modulate the brightness, contrast, and clarification.

Also, 3D image of cells on fibers in the single and three layers was collected using a confocal microscope (Leica TCS SP II, Heidelberg, Germany). Image stacks of both single and three layers along the z-axis were collected at a step size of 1.282 μm for single-layer cultures and 4.271 μm for three-layer cultures. The observed thickness of the z-axis for single and three layers were 30.77 and 89.70 μm , respectively. At each step, the two fluorescent signals of nuclei and skeletal actin and one light signal of fibers were collected. Then, fluorescent and light signals of cells on fibers in the single layer at 15.36 μm in z-axis were overlapped. To obtain 3D hologram, fluorescence signals of cells at each step were merged in the three-layer.

Samples were also analyzed using SEM to evaluate the distribution of fibers and cells. For this purpose, samples were dried using ethanol and analyzed similar to the fibers described above (Section 2.3.).

2.7. Histology assay

30 days after cell culture, the samples formed using single and three layers of fibers were tailored using a tweezer and scissors. The aluminum frames of the samples were completely removed. Random parts of the samples were fixed in 3.7% formaldehyde, dried through an ethanol gradient, and embedded in paraffin. The samples were cut into 4 μm and stained with hematoxylin and eosin (H & E) for histology analysis [20].

3. RESULTS

3.1. Fabrication of the thin layer of highly porous fibers

Conventional electrospray setup consists of a syringe pump, syringe and a needle of appropriate size, high voltage power supply, earth grounding, and a stationary collector plate (Figure 1A). The collector plate is a flat conducting plate where the polymer fibers accumulate. After certain elution volume, the fibers are removed and used in the needed application. To remove the material, larger volumes are deposited which leads to fibrous structures with limited pore size. We questioned whether the fibers can be accumulated by creating a hole in the collector plate. For this purpose, different size holes were created in wood, plastic or glass, and wrapped around with a conductive aluminum foil (Figure 1B), which can be autoclaved when sterilization is necessary. The collector plate was designed with the intention of using it as a support structure

while transporting and subsequent handling. Experiments performed at the same conditions as the traditional collector plate showed the presence of fibers in the holed area, suggesting the possibility of forming thin layers. Different shapes such as circle, hexagon and rectangle with varying sizes (up to 10 cm) were tested. These results showed the possibility of obtaining thin layers. Since the aluminum foil could be simply peeled off from the core structure, it is also easy for the thin layer to be handled without mechanical damage from external stress.

Absence of the continuous conducting medium could alter the electrical field. Hence, we questioned how the distribution of fibers would be altered and whether the formed fibers have different architecture. Similar to other reports, fibers generated by the conventional plate showed multiple layers of fibers (Figure 3A) under scanning electron microscopy. However, few layers of fibers were observed in the open area of the new collector plate, (Figure 3B) while multiple layers were observed on the sheet. Many fiber morphologies appeared smooth and similar between the two conditions, except in case of a large fiber; in the conventional plate (Figure 3A), many fibers showed pores on their surface. To test whether nanosize fibers could be obtained using the new collector plate, processing parameters were optimized by manipulating the flow rate of the solution, the strength of voltage, and the distance between the needle tip and the collector. The conventional collector plate showed multilayered nanofibers (Figure 3C). Similar nanofibers were collected on the new collector plate with a single layer (Figure 3D), suggesting the applicability of this collector plate to other conditions.

To test whether the new collector plate is applicable to other polymeric systems, forming fibers using naturally derived gelatin was tested. These results showed that the gelatin fibers accumulated similar to the PCL fibers (Figure 3E). Others have also used sequential (exchanging the syringes containing two different polymeric solutions in sequence) and simultaneous (using two syringes containing two different polymeric solutions at the same time) process of electrospaying to deposit two different polymers for controlling the microarchitecture [21–24]. To test this possibility, PCL and gelatin were deposited sequentially or simultaneously. These results showed (Figure 3F) that thin layers of fibers of different polymers can be collected on the novel collector plate.

To understand the effect of hydration on the fibers, formed fibers were observed under light microscopy before and after hydration. Upon hydration in phosphate buffered saline (PBS), the PCL fiber structure remained the same. However, gelatin fibers completely dissolved in PBS as they were not stabilized by any cross-linker. When composite structures were hydrated, PCL fibers still remained intact even after thirty or more days. However, the fibers made of PCL and gelatin were entangled and collapsed within 15 minutes because gelatin dissolved in PBS. Thus, one could easily understand the alterations in fibrous architecture using these thin layers.

3.2. Fiber characterization

To understand the fiber size and pore size, fibers were generated under the same condition of solution (concentration of solution) and process parameters (flow rate, needle size, distance between the needle tip and the collector, and high voltage supply) using the novel and the conventional collector plates. Quantification of scanning electron micrographs showed that the new collector plate does not affect the fiber size and the shape of the pores in the scaffolds (Figure 4A). Even when nanofibers were formed at another condition, no significant difference was obtained. Thus, this new collector plate can be easily adapted to various other polymers in conjunction with the intended application. Controlling fiber sizes is also possible using appropriate solvents and the distance of the collector plate. This suggests that the technology is versatile and can be easily integrated into existing technologies. The shape factor (Figure 4B) of pores formed due to random distribution of fibers were similar in both cases.

Pore size (Figure 4C) of the scaffold formed with the new collector plate showed significant increase due to the decreased density of fibers deposited in the open area. However, under the same conditions of solution and process parameters, the diameter of fibers generated by the novel and conventional fibers were quite similar. The pore size of fiber produced with the novel collector is much greater than those produced with the conventional one.

Collected fibrous structures at the same condition for the same time were tested under tensile loading in the dry state at room temperature. Load-extension curves (Figure 4D) showed that the extension of novel fibers was twice as long as that of conventional fibers; novel fibers showed 250% strain where as the conventional fibers showed 100% strain. However, the load carrying capacity by the fibrous structures were nearly half that of conventional fibers. These differences could be attributed to the decreased density of fibers in the novel collector plate; due to free space between the fibers on the sample, thin layers can stretch but cannot carry too much load.

3.3. Developing 3D colonized cells

To test whether cells can be cultured on these thin layers, formed porous structures along with the aluminum foil were inserted onto albumin-coated (to minimize cell adhesion to the tissue culture plastic) seeded with HFF-1 cells. For evaluating layer-by-layer assembly, the process of inserting the thin layer and seeding cells was done three times (Figure 2). Entire assembly was cultured for seven days in serum containing medium with the routine monitoring under light microscopy. An increase in the number of cells was observed on fibers in single and three layers. Further, many cells in both single and three layers appeared in clusters at the initial time point, but showed spreading and a spindle shape. By day 7, a number of pores were covered with the regenerated components. To assess the cellular components, they were stained for cytoskeletal actin and counterstained for nucleus using DAPI. To avoid background fluorescence signal from cells on the surface of cell culture dish, the samples were moved into new dishes after the staining and washing. Fluorescent images (Figure 5) in single or three layers showed a qualitative improvement in the cells up to 7 days. Moreover, cells were individually distributed and surrounded by matrix elements, suggesting that the cells are functional. In addition, some cells were focused in the plane of view and others were unfocused, as they are attached in different layers of fibers.

To better understand the distribution of cells in three-dimension, confocal microscopic analysis was performed using a step size of 1.2821 μm . Reconstructed confocal images of three layers showed presence of cells in every layer in 89.7 μm thickness of three layer culture (Figure 6). In a single layer culture, more cells appeared as they are distributed in a narrow thickness. To assess the distribution of cells in relation to fibers, light microscopy image in the same plane was overlaid with fluorescent images. An obtained micrograph showed that cells were surrounded by fibers and attached to the fibers, particularly in pores which were not too large relative to the size of cells. Note that Figure 6H is a 3D image which can be better visualized using a 3D-spectacle. This suggested that cells are distributed continuously in three-dimension.

Samples were also evaluated using SEM to understand distribution of cells within the fibers. These results revealed (Figure 7A) that the cells on all fibers attachment to the fibers and were entangled by the fibers. Cells attached and spread throughout the matrix. In some locations, cells showed numerous lamellapodia and filapodia with anchorage points to the fibers (Figure 7B), probably via the adhesion of serum proteins to the polymeric matrix. However, in many locations individual cells could not be identified, probably due to the presence of secreted matrix elements. Cells grew through fibers and the thickness of fibers increased. Cell clusters were observed both vertically and horizontally, covering several fibers. This suggests that cells grew due to a thin layer of electrospayed fibers with large pore sizes.

3.4. Cell-glued 3D scaffold

To confirm whether three layers of fibers were attached after a 7 day cell culture, the sample was lifted by a tweezer but the bottom layer of the sample was detached from the sample (Figure 8A). Moreover, the sample disappeared while cutting by scissors because the complexity of the fibers and cells was still weak mainly due to a fragile structure of fibers (Figure 8B). When cell cultures were continued up to 30 days, three layers merged into a single structure, probably due to the regeneration of matrix elements and cell growth (Figure 8C). Moreover, the shape of the 3D scaffold was stable and tailorable without the deformation of the scaffold while and after the scaffold was cut by scissors (Figure 8D).

The samples were cut into small random pieces for further analyses by SEM and histology. The dry thickness of the 3-layered assembly was 280 μ m using SEM (not shown here). Clustered cells existed on the top and side of the 3D scaffold. HFF-1 cells were distributed throughout the scaffold not only vertically but also horizontally and this well distribution supports the complex structure of cells and fibers without any mechanical damage even after cutting into the small pieces for H & E staining (Figure 8E and 8F). Cells grew on the surface of fibers. HFF-1s wrapped around a single fiber and elongated along the fiber. These cells attached adjacent cells growing on another nearby fiber not only vertically but also horizontally. The cells were distributed throughout in all dimensions of the scaffold without any distinguishable layers between cells and fibers. This complex structure of fibers and cells in three layers glued three layers into one 3D scaffold after 30 days, to tailor the shape of the scaffold, and to cut into small pieces without any mechanical damage. Thus, the cells glued 3D scaffold was fabricated using the thin layer of PCL fibers, and HFF-1 in 15% serum added media after 30 day cell culture as a phenotype of 3D scaffold using electrospayed fibers with large pore size.

4. DISCUSSION

Biodegradable scaffolds are used to support and guide the in-growth of cells and the scaffolding material eventually disappears leaving only the necessary healthy tissue in a topologically required form. This study demonstrated the possibility of i) developing very thin layers of fibers from different polymers, ii) handling them in tissue culture conditions, and iii) building multiple layers of cells and fibers. Cells attach and distribute in 3D synthetic polymer PCL. Since the technology is simple for the novel collector to be associated with existing techniques of electrospinning for a number of other biomaterials. The thin layer of electrospayed fibers is easy to handle without mechanical damage due to the support of an aluminum frame. Even when fibers were handled for the morphology study, the polymeric structures of the fibers remained intact, suggesting their ability to endure outside stress. Without directly grabbing the fragile fibers, the aluminum foil provides a hard frame for the thin layers of the fibers to be picked up with tweezers and preventing the fibers from being destroyed.

The pore size of fibers produced with the new collector plate are larger than those produced with conventional collectors due to the decreased density of fibers. However, the diameter of fibers under the same conditions are similar and can be manipulated by controlling solution (concentration of polymer solutions, solvent) and process parameters (flow rate, needle tip, distance between tip and collector, and high voltage supply). Thus, the larger pore size of fibers were generated while the diameter of fibers were controlled by using the collector. In other words, the innovative technique of the collector is easy to combine with the existing technology of electrospaying or electrospinning.

This study opens a new window of opportunity to understand a number of cellular interactions in 3D environment, mimicking physiological conditions. For example, a single layer can be visualized in a regular light microscope and the presence of fibers creates a rough architecture

similar to a physiological environment. Thus, a single layer can also be used in cell culture to study the interactions in single cells in 3D space. Traditional tissue culture conditions can be converted into 3D cultures without significant effort. Thin layers can be placed serially to develop thick 3D structures by adapting layer-by-layer assembly. One could build tissues to the required thickness layer-by-layer.

SEM images of cells cultured on fibrous scaffolds fabricated using electrospinning showed that the cells can grow and proliferate within the fibrous scaffold. The cells were growing on fibers and were intertwined with the fibers. This novel collector overcame barriers of electrospayed and electrospun fibers. The majority of fibers made by the existing technology showed that the pore sizes between the fibers were not proper for cells to infiltrate into the pore between and among fibers. It was demonstrated that HFF-1 cells grew and proliferated when cultured onto scaffolds made of thin layers of fibers fabricated by electrospaying using a novel collector. In addition, the single layer of electrospun fibers were expanded up to three layers. Further, the layer-by-layer assembly also helps solve problems associated with the uniform seeding of cells into the porous structure, typically observed in many scaffolds synthesized by subtractive techniques such as porogen-leaching and freeze drying. Moreover, cells in the 3D scaffold grew and became distributed throughout the sample, not only horizontally but also vertically, suggesting that diffusion of media was sufficient for cells to functionalize in the three layers. Thus, two core techniques of a thin layer of electrospayed fibers with large pore sizes and layer-by-layer assembly, are a synergistic effect on overcoming current barriers such as thicker tissue regeneration.

In this study, PCL was used to demonstrate the concept of cell colonization on thin layers, which does not have a cell binding domain. Much of the cell adhesion is due to the interaction with the serum proteins, as cells were cultured in 15% serum containing media. To better understand the cellular interactions with fibers, changes in adsorption of serum protein needs to be measured [25]. The cell glued 3D scaffolds demonstrated that cells in three layers were functional and well distributed in the sample. However, a thicker 3D scaffold study using four or more layers needs to clarify the limitation of media diffusion. When the limitation becomes clear, a new reactor design needs to allow cells to functionalize in thicker 3D scaffolds. Not only that, analysis of cellular activity needs to be extended to include other types and functionality; assembly and maturation of matrix elements in tissue regeneration plays a significant role in determining the biomechanics and the quality of the regenerated tissue. In addition, evaluating alteration in cellular activity after immobilizing proteins containing cell adhesion domains could provide more information on the importance of fiber thickness and roughness. Recent advances in tissue regeneration, 3D matrix physical properties such as hydrophilicity, stiffness [26], porosity [27], pore size and void fraction can affect cell morphology, attachment and function. Also, cellular activity is influenced by scaffold stiffness [28–30]. Cells show reduced spreading and disassembly of actin even when soluble adhesive ligands are present in weak gels [31–32]. Maximum tractional force generated by a cell could be as much as 10–15% of substrate modulus [31]. Further, the rigidity of the scaffolds may affect the formation of ECM which can affect cellular activity [33]. We performed bulk tensile properties. However, to understand the influence of scaffold stiffness, properties of individual fibers need to be analyzed using techniques such as nanoindentation. In addition, the influence of fiber curvature on cell colonization also needs to be analyzed.

This study focused on using thin layers of electrospayed fibers in tissue regeneration. This technique could also be used in numerous other applications such as chemical and biochemical protection in defense and security, solar cells and fuel cells in sustainability, membranes and filters in environmental engineering and biotechnology [34].

5. CONCLUSION

In summary, the novel collector plate allows the formation of thin layers of electrosprayed fibers with large pore sizes. The thin layer of electrosprayed fibers can be easily handled without mechanical damage because of the supporting structure. This collector is also versatile enough to be associated with existing techniques of electrospinning to manipulate mechanical and biological properties of novel fibers. This methodology overcame the major barrier of the electrospinning technique and its application for tissue regeneration. The novel fibers allow a single cell study on single fibers in a single layer, and in multilayer by using a layer-by-layer technique. Furthermore, Cell glued 3D scaffold of the thin layer of electrosprayed fibers with large pore sizes will expand its implications on other cells, fibers, tissues and organs.

Acknowledgments

Thanks to Dr. James Smay, Dr. Charlotte Ownby, and Mr. Curtis Andrew for their help on using SEM, confocal microscope, and H & E staining. Financial support was provided by the National Institutes of Health (1R21DK074858).

References

1. Langer R, Vacanti JP. Tissue engineering. *Science* 1993;260:920–6. [PubMed: 8493529]
2. Tissue engineering. *Nature Biotechnology*. 2000. p. IT56-IT8.
3. Vyavahare N, Ogle M, Schoen FJ, Zand R, Gloeckner DC, Sacks M, et al. Mechanisms of bioprosthetic heart valve failure: fatigue causes collagen denaturation and glycosaminoglycan loss. *J Biomed Mater Res* 1999;46:44–50. [PubMed: 10357134]
4. Chvapil M. Collagen sponge: theory and practice of medical applications. *Journal of Biomedical Materials Research* 1977;11:721–41. [PubMed: 893491]
5. Oberpenning F, Meng J, Yoo JJ, Atala A. De novo reconstitution of a functional mammalian urinary bladder by tissue engineering. *Nat Biotechnol* 1999;17:149–55. [PubMed: 10052350]
6. Madihally SV, Matthew HW. Porous chitosan scaffolds for tissue engineering. *Biomaterials* 1999;20:1133–42. [PubMed: 10382829]
7. Mikos AG, Thorsen AJ, Czerwonka LA, Bao Y, Langer R, Winslow DN, et al. Preparation and characterization of poly(L-lactic acid) foams. *Polymer* 1994;35:1068–77.
8. Mooney DJ, Baldwin DF, Suh NP, Vacanti JP, Langer R. Novel approach to fabricate porous sponges of poly(D,L-lactic-co-glycolic acid) without the use of organic solvents. *Biomaterials* 1996;17:1417–22. [PubMed: 8830969]
9. Wang YC, Ho CC. Micropatterning of proteins and mammalian cells on biomaterials. *Faseb J* 2004;8:8.
10. Hutmacher DW. Scaffolds in tissue engineering bone and cartilage. *Biomaterials* 2000;21:2529–43. [PubMed: 11071603]
11. Morton, WJ. Method of dispersing fluids US Patent. 1902;705691.
12. Sill TJ, von Recum HA. Electrospinning: Applications in drug delivery and tissue engineering. *Biomaterials* 2008;29:1989–2006. [PubMed: 18281090]
13. Shin H, Jo S, Mikos AG. Biomimetic materials for tissue engineering. *Biomaterials* 2003;24:4353–64. [PubMed: 12922148]
14. Nisbet DR, Forsythe JS, Shen W, Finkelstein DI, Horne MK. Review Paper: A Review of the Cellular Response on Electrospun Nanofibers for Tissue Engineering. *J Biomater Appl*. 2008 0885328208099086.
15. Fibrous 3-dimensional scaffold via electrospinning for tissue regeneration and method for preparing the same. USPTO; 2008. p. 0233162
16. Stankus JJ, Soletti L, Fujimoto K, Hong Y, Vorp DA, Wagner WR. Fabrication of cell microintegrated blood vessel constructs through electrohydrodynamic atomization. *Biomaterials* 2007;28:2738–46. [PubMed: 17337048]
17. Mondalek FG, Lawrence BJ, Kropp BP, Grady BP, Fung KM, Madihally SV, et al. The incorporation of poly(lactic-co-glycolic) acid nanoparticles into porcine small intestinal submucosa biomaterials. *Biomaterials* 2008;29:1159–66. [PubMed: 18076986]

18. Sarasam A, Madihally SV. Characterization of chitosan–polycaprolactone blends for tissue engineering applications. *Biomaterials* 2005;26:5500–8. [PubMed: 15860206]
19. Pok SW, Wallace KN, Madihally SV. In vitro characterization of polycaprolactone matrices generated in aqueous media. *Acta Biomater* 2010;6:1061–8. [PubMed: 19664731]
20. Madihally SV, Solomon V, Mitchell RN, Van De Water L, Yarmush ML, Toner M. Influence of insulin therapy on burn wound healing in rats. *J Surg Res* 2003;109:92–100. [PubMed: 12643849]
21. Gupta P, Wilkes GL. Some investigations on the fiber formation by utilizing a side–by–side bicomponent electrospinning approach. *Polymer* 2003;44:6353–9.
22. Hellmann C, Belardi J, Dersch R, Greiner A, Wendorff JH, Bahnmüller S. High Precision Deposition Electrospinning of nanofibers and nanofiber nonwovens. *Polymer* 2009;50:1197–205.
23. Kidoaki S, Kwon IK, Matsuda T. Mesoscopic spatial designs of nano– and microfiber meshes for tissue–engineering matrix and scaffold based on newly devised multilayering and mixing electrospinning techniques. *Biomaterials* 2005;26:37–46. [PubMed: 15193879]
24. Varesano A, Carletto RA, Mazzuchetti G. Experimental investigations on the multi–jet electrospinning process. *Journal of Materials Processing Technology* 2009;209:5178–85.
25. Tillman J, Ullm A, Madihally SV. Three–dimensional cell colonization in a sulfate rich environment. *Biomaterials* 2006;27:5618–26. [PubMed: 16884767]
26. Balgude AP, Yu X, Szymanski A, Bellamkonda RV. Agarose gel stiffness determines rate of DRG neurite extension in 3D cultures. *Biomaterials* 2001;22:1077–84. [PubMed: 11352088]
27. Dar A, Shachar M, Leor J, Cohen S. Optimization of cardiac cell seeding and distribution in 3D porous alginate scaffolds. *Biotechnol Bioeng* 2002;80:305–12. [PubMed: 12226863]
28. Zaleskas JM, Kinner B, Freyman TM, Yannas IV, Gibson LJ, Spector M. Growth factor regulation of smooth muscle actin expression and contraction of human articular chondrocytes and meniscal cells in a collagen–GAG matrix. *Exp Cell Res* 2001;270:21–31. [PubMed: 11597124]
29. Lee CR, Grodzinsky AJ, Spector M. The effects of cross–linking of collagen–glycosaminoglycan scaffolds on compressive stiffness, chondrocyte–mediated contraction, proliferation and biosynthesis. *Biomaterials* 2001;22:3145–54. [PubMed: 11603587]
30. Sieminski AL, Hebbel RP, Gooch KJ. The relative magnitudes of endothelial force generation and matrix stiffness modulate capillary morphogenesis in vitro. *Exp Cell Res* 2004;297:574–84. [PubMed: 15212957]
31. Lo CM, Wang HB, Dembo M, Wang YL. Cell movement is guided by the rigidity of the substrate. *Biophys J* 2000;79:144–52. [PubMed: 10866943]
32. Pelham RJ Jr, Wang Y. Cell locomotion and focal adhesions are regulated by substrate flexibility. *Proc Natl Acad Sci U S A* 1997;94:13661–5. [PubMed: 9391082]
33. Wozniak MA, Modzelewska K, Kwong L, Keely PJ. Focal adhesion regulation of cell behavior. *Biochim Biophys Acta* 2004;1692:103–19. [PubMed: 15246682]
34. Ramakrishna S, Fujihara K, Teo W-E, Yong T, Ma Z, Ramaseshan R. Electrospun nanofibers: solving global issues. *Materials Today* 2006;9:40–50.

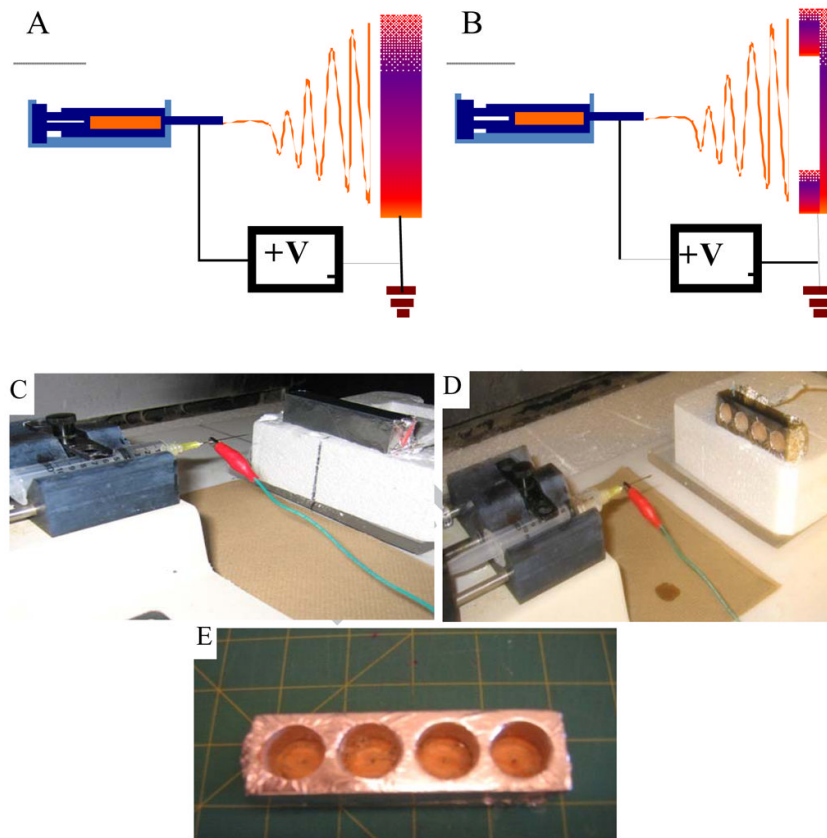


Figure 1. Novel electro spray setup

(A) Schematic representation of conventional electro spray setup (B) Schematic representation of novel electro spray setup. (C) Photograph of conventional electro spray setup and (D) Photograph of novel electro spray setup. (E) Photograph of the novel collector.

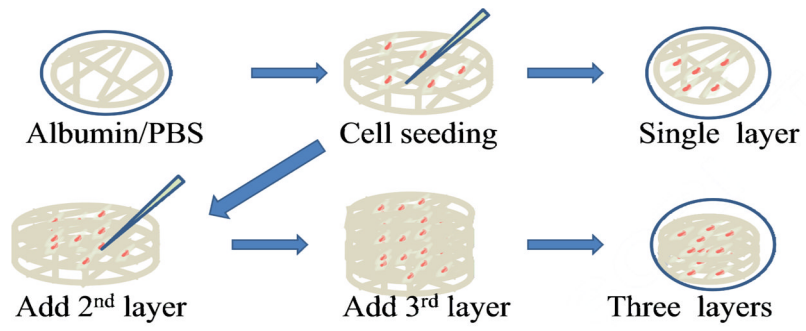


Figure 2. Schematic of the process of cell seeding using layer-by-layer assembly.

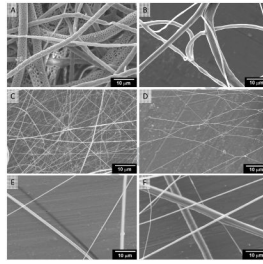


Figure 3. Morphology of fibers using novel and conventional collectors

Microfibers made of PCL (M_w 43000) with (A) conventional collector and (B) novel collector at the same condition. Nanofibers made of PCL ($M_w=43000$) with (C) conventional collector and (D) novel collector at the same condition. (E) Fibers made of Gelatin Type A using the novel collector. (F) Hybrid fibers made of microsize PCL ($M_n=80000$) fibers and nanosize Gelatin Type A fibers in sequential process using the novel collector.

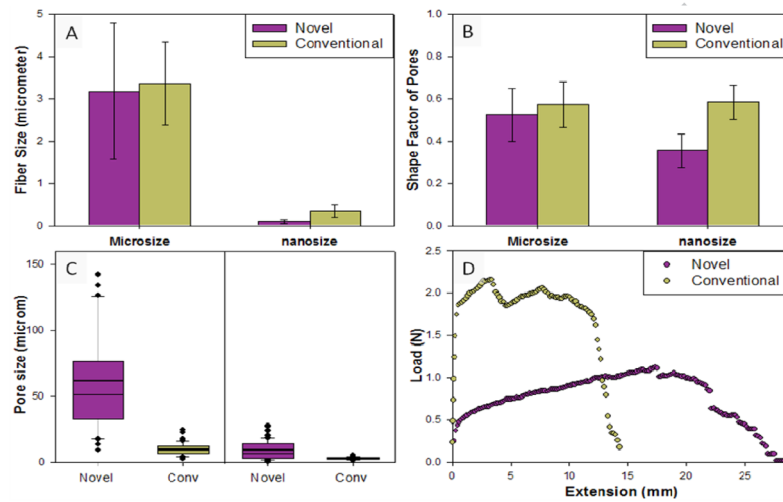


Figure 4. Comparison of fibrous layer characteristics
(A) Fiber diameters and the error bars correspond to the standard deviation ($n = 50$). **(B)** Shape factor and the error bars correspond to the standard deviation ($n = 50$). **(C)** Box plot showing the distribution of pore size with 10th, 25th, 50th, 75th, and 90th percentiles and the mean value (thick line within each box). Values that were outside 95th and 5th percentiles were treated as outliers. **(D)** The load–extension behavior.

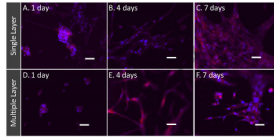


Figure 5. Cell colonization in thin layers using layer-by-layer assembly
(A–C) Fluorescent micrographs of cells on single layer of fibers. (D–F) Fluorescent micrographs of cells on three layers of fibers. The samples were stained with Alexa phalloidin for cytoskeletal actin (red) and counterstained with DAPI for nuclei (blue) of cells. Scale bar corresponds to 50 μm .

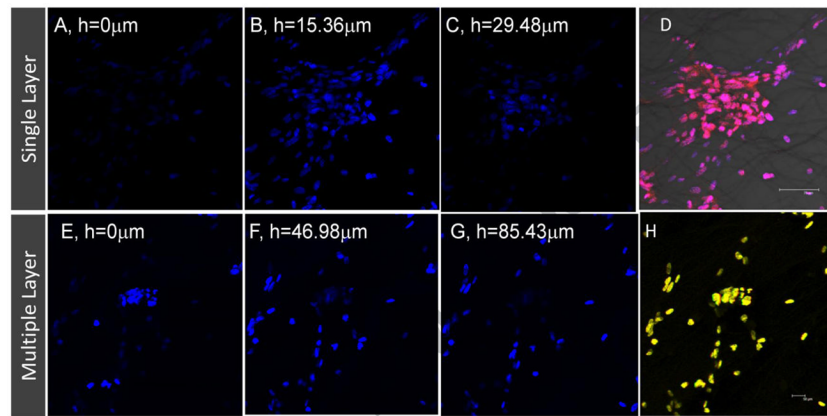


Figure 6. Cell distribution on different heights of the fibrous assembly at day 7
(A–C) The nuclei of cells on fibers at different heights in single layer. (D) Overlaid image of fluorescence and light signals from cells and electrospayed fibers in the single layer at 15.36 µm. (E–G) The nuclei of cells on fibers at different heights in the three layers. (E) Compilation of images in different planes showing distribution of cells in three-layers, best seen using 3D spectacles.

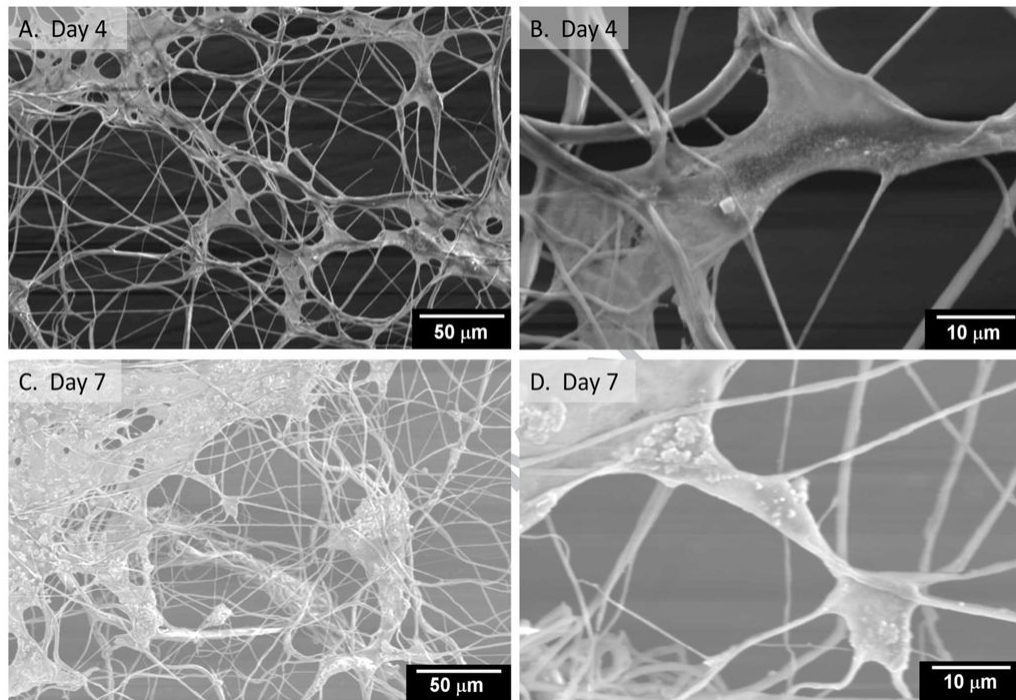


Figure 7.
Morphology of cells in single layer of fibers by SEM.

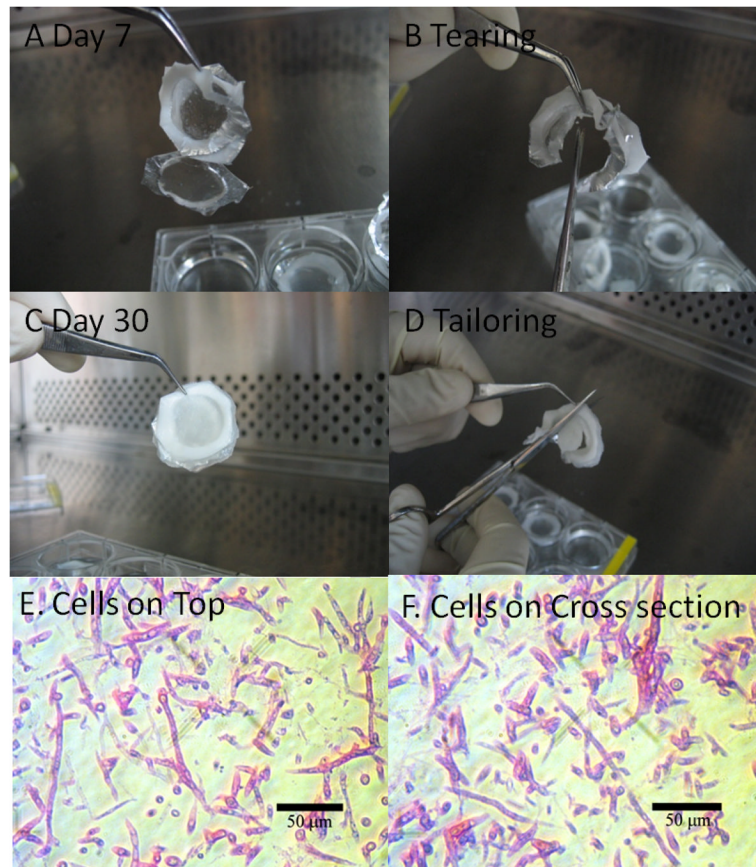


Figure 8. Cell glued 3D scaffolds

(A) Three layers of fibers after cell culture of 7 days (B) Collapsing three layers while cutting after cell culture for 7 days (C) Cell glued three layers of fibers after cell culture of 30 days (D) Tailoring tissue-like materials after cell culture of 30 days. (E–F) Cell morphology after cell culture for 30 days using top area and cross section of three layers stained with H & E for nuclei (red) and cytoplasm (dark pink).